

Effects of deposition temperature on the structural, electrical and magnetic properties of $\text{Mn}_{1.56}\text{Co}_{0.96}\text{Ni}_{0.48}\text{O}_4$ spinel films grown on YSZ (100) substrates by pulsed laser deposition

ZHANG Tao-Lue^{1,2}, LIU Fang¹, LIN Tie², XU De-Cai^{1,2}, HOU Yun^{2*}

- (1. School of Materials Science and Engineering, University of Shanghai for Science and Technology, Shanghai 200093, China;
2. State Key Laboratory of Infrared Physics, Shanghai Institute of Technical Physics, Chinese Academy of Sciences, Shanghai 200083, China)

Abstract: $\text{Mn}_{1.56}\text{Co}_{0.96}\text{Ni}_{0.48}\text{O}_4$ (MCNO) thin films with spinel structure were grown on YSZ (100) substrates at different deposition temperatures from 500 °C to 700 °C by pulsed laser deposition. Since the deposition temperature is an important factor in fabricating high-quality films, the structural, electrical and magnetic properties of MCNO thin films as a function of deposition temperature are investigated. By analyzing the X-ray diffraction patterns and the atomic force microscopy images, it is discovered that the crystallization of MCNO films is highly dependent on the deposition temperature. With the increasing deposition temperature, the resistivity of MCNO thin films is a change of V-type, and the electrical conduction of the MCNO films is controlled by a small polaron hopping mechanism. Meanwhile, the temperature-dependent magnetization curve reveals that all the samples show ferromagnetism to paramagnetism transition and the MCNO film deposited at 600 °C has a high Curie temperature of 216 K. All the results above demonstrate that MCNO film deposited at 600 °C has satisfactory performance, which is desirable for applications of thermistor devices and multifunctional heterojunctions.

Key words: thin film technology, pulsed laser deposition, deposition temperature, magnetic properties

PACS: 75. 70. -i, 68. 55. -a

沉积温度对脉冲激光沉积法在 YSZ (100) 衬底上生长 $\text{Mn}_{1.56}\text{Co}_{0.96}\text{Ni}_{0.48}\text{O}_4$ 尖晶石薄膜结构、电学和磁学性能的影响

张韬略^{1,2}, 刘芳¹, 林铁², 徐德才^{1,2}, 侯云^{2*}

- (1. 上海理工大学材料科学与工程学院, 上海 200093;
2. 中国科学院上海技术物理研究所 红外物理国家重点实验室, 上海 200083)

摘要: 在 YSZ(100) 衬底上, 采用脉冲激光沉积法在 500 °C 至 700 °C 的不同沉积温度下生长出尖晶石结构的 $\text{Mn}_{1.56}\text{Co}_{0.96}\text{Ni}_{0.48}\text{O}_4$ (MCNO) 薄膜。由于沉积温度是制备高质量薄膜的重要因素, 因此本文研究了 MCNO 薄膜结构、电学和磁学性能随沉积温度的变化。通过对 X 射线衍射图和原子力显微镜图像的分析, 发现 MCNO 薄膜的结晶与沉积温度有很大关系。随着沉积温度的升高, MCNO 薄膜的电阻率呈 V 型变化, 其导电过程可以用小极化子跳跃机理来描述。同时, 随温度变化的磁化曲线表明所有样品都显示出从铁磁性到顺磁性的转变, 且沉积温度为 600 °C 的 MCNO 薄膜具有 216 K 的高居里温度。以上研究结果表明, 在 600 °C 沉积的 MCNO 薄膜具有适用于热敏电阻器件和多功能异质结所需的良好性能。

关键词: 薄膜技术; 脉冲激光沉积; 沉积温度; 磁学性能

中图分类号: O484.1; O484.4 + 2 文献标识码: A

Received date: 2020- 02- 05, revised date: 2020- 09- 09

收稿日期: 2020- 02- 05, 修回日期: 2020- 09- 09

Foundation items: Supported by National Natural Science Foundation of China (61275111)

Biography: ZHANG Tao-Lue (1995-), male, Gansu China, Master. Research area involves new infrared detection materials and devices
E-mail: ztl1754355048@163. com

* Corresponding author: E-mail: hyun@mail. sitp. ac. cn

Introduction

$\text{Mn}_{1.56}\text{Co}_{0.96}\text{Ni}_{0.48}\text{O}_4$ thin film with spinel structure has attracted considerable interest because of its high negative temperature coefficient (NTC), fast response and high Curie temperature^[1-3]. It has been widely used in optoelectronics devices, thermal detectors, and functional spintronics devices^[4-6].

Numerous preparation techniques for the MCNO thin films have been conducted over the past few years, such as chemical solution deposition (CSD), pulsed laser deposition (PLD), radio frequency magnetron sputtering, laser molecular beam epitaxy (LMBE), and so forth^[6-9]. Compared with other technologies, the process parameters of PLD can be precisely adjusted, and no limit applies to the target types. In addition, short deposition cycle and uniform prepared film contribute to the advantages of PLD method, therefore, a multi-component film with desired stoichiometric ratio can be obtained with ease^[2, 7, 10-12]. It has been reported that the resistivity of MCNO films decreases as the deposition temperature increases from 50 °C to 250 °C by PLD method^[13]. The effects of growth temperature on NTC characteristics of MCNO films by LMBE were studied^[9, 14]. The MCNO films grown at 500 °C by LMBE method exhibited excellent electrical properties^[15]. With the increase of growth temperature, the grain size, Curie temperature and magnetic moment of MCNO films prepared by CSD method increase, while the resistance decreases^[6, 16]. Though the structural, electrical and optical properties of MCNO have been extensively studied^[3, 13-18], effort in researching on magnetic properties, especially its correlation with other characters, is lacking. Therefore, the relationship between structural property and magnetic property of the MCNO thin films at different deposition temperatures needs to be studied in detail.

In this paper, we report the MCNO thin films prepared on YSZ (100) substrates by the PLD method. The deposition temperature was set from 500 °C to 700 °C. The influences of deposition temperature on the structural, electrical and magnetic properties of MCNO thin films were investigated, which is significant to the applications of MCNO films.

1 Experiments

As starting materials, manganese acetate ($\text{Mn}(\text{CH}_3\text{COO})_2 \cdot 4\text{H}_2\text{O}$), cobalt acetate ($\text{Co}(\text{CH}_3\text{COO})_2 \cdot 4\text{H}_2\text{O}$) and nickel acetate ($\text{Ni}(\text{CH}_3\text{COO})_2 \cdot 4\text{H}_2\text{O}$) were weighed with an atomic ratio of $\text{Mn}:\text{Co}:\text{Ni} = 52:32:16$, and then dissolved completely in water. Solid powder could be obtained by the thermal evaporation method. Afterwards, the target wafer with a size of 20 mm in diameter and 4 mm in thickness was prepared after sintering.

YSZ (100) substrates were pretreated by ultrasonic cleaning in the order of acetone, alcohol and deionized water. The substrates were annealed at 700 °C for 5 min to eliminate residual stress. The process parameter settings of the PLD system were listed as follows; KrF excimer laser, 248 nm wavelength, 30 ns pulse width, 1.5

$\text{J}\cdot\text{cm}^{-2}$ power density, and the deposition repetition was 3 Hz. The distance of substrate-to-target was kept as 40 mm, and the deposition temperature range was selected from 500 °C to 700 °C. The chamber pressure was evacuated to about 0.5×10^{-5} Pa, the oxygen was then injected into the cavity with the oxygen partial pressure being kept at 6×10^{-2} Pa during the deposition process. All the films were deposited for 80 min so that the film thickness was around 80 nm. After the deposition, the MCNO films were naturally cooled to room temperature in the PLD vacuum chamber, and annealed at 750 °C for 10 min in the air by rapid thermal processing.

The crystallization of the films was identified by X-ray diffraction (XRD) using a Rigaku D/MAX-2550 X-ray diffractometer with Cu K α radiation at 40 kV and 25 mA. The surface morphologies of the thin films were investigated by a Nanoscope IIIa multimode atomic force microscope (AFM) (Bruker, Santa Barbara, CA) using tapping mode. The electrical properties of the films were measured in the temperature range of 180 K to 310 K by the affiliated temperature controlling systems and Keithley 2400 source meter in the vacuum cavity. Magnetic properties of the films were measured at field cooling (FC) mode from 50 K to 310 K under 10000 Oe using a vibrating sample magnetometer (VSM) which was equipped in a physical properties measurement system (PPMS-9, Quantum Design).

2 Results and discussions

2.1 Structural and morphological properties

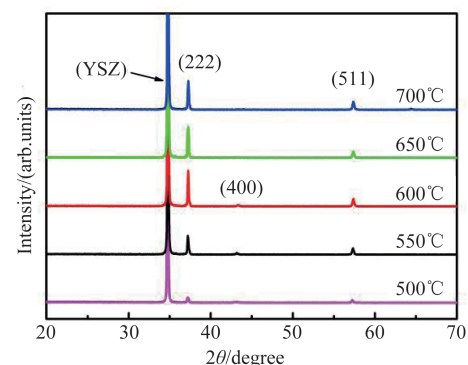


Fig. 1 XRD patterns of MCNO films prepared at different deposition temperatures.

图1 在不同沉积温度制备的MCNO薄膜的XRD图谱

The XRD patterns of the MCNO thin films prepared at different deposition temperatures are demonstrated in Fig. 1. As can be seen, the crystallization of MCNO films highly depends on the deposition temperature. It can be noticed that all the samples have (511) and (222) diffraction peaks, which proves that these films exhibit a spinel structure. When the deposition temperature is lower than 600 °C, the intensity of (222) diffraction peak increases with the increase of temperature, which is indicative of that the crystallinity of the MCNO films is improved. During the course of

deposition, the atoms collected on the substrate gained the thermal energy, and the surface mobility and surface diffusion of the atoms were enhanced, which resulted in the islands nucleation and growth^[19-20]. However, when the deposition temperature increases to more than 600 °C, the intensity of the diffraction peak declines.

To measure the crystal quality of the films deposited at different temperatures, the 3D AFM images are displayed in Fig. 2. It can be seen clearly that the grains of the MCNO films deposited at 500 °C are small and uniform, and the grains start to grow with the increase of deposition temperature. Compared with other samples, the film deposited at 600 °C has the largest number of large-grains per unit area, which proves that the deposition temperature can affect the growth of grains in the process of deposition. However, the number of large grains is reducing at higher temperatures. It can be explained by the grain cracking and the formation of twin crystal of MCNO film at higher temperature^[21-22].

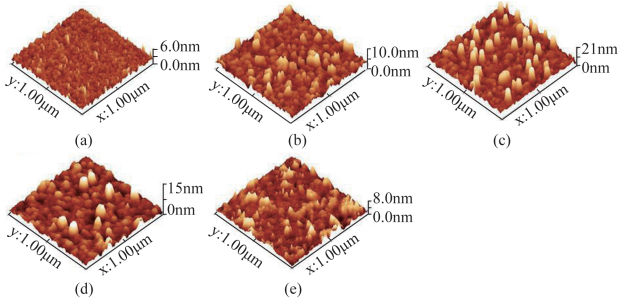


Fig. 2 AFM images of MCNO films deposited at (a) 500 °C, (b) 550 °C, (c) 600 °C, (d) 650 °C, (e) 700 °C

图2 不同温度沉积的MCNO薄膜的AFM图(a) 500 °C, (b) 550 °C, (c) 600 °C, (d) 650 °C, (e) 700 °C

2.2 Electrical properties

The relations between electrical resistivity ρ and temperature T of MCNO films are displayed in Fig. 3. It is noticeable that when the deposition temperature increases from 500 °C to 600 °C, the corresponding resistivity of the samples decreases. The inset of Fig. 3 manifests the electrical resistivity testing at 300 K of samples deposited at different temperatures. This indicates that the deposition temperature has an important influence on the resistivity of MCNO films. The resistivity reaches a minimum of 454.38 $\Omega \cdot \text{cm}$ at 600 °C, and then increases when the temperature climbs to 700 °C. The resistivity is lower than the results (920~3 539 $\Omega \cdot \text{cm}$) reported by the Kong^[13] at low deposition temperature (50~250 °C) by PLD method. The electrical properties of MCNO films are closely related to their crystallinity. The large number of large-grains of MCNO films deposited at 600 °C means that the number of insulating grain boundaries is small, which leads to a low resistivity^[16].

The figure of temperature versus electrical resistivity is indicative of NTC thermistor characteristics, which can be described by the general expression for small polaron hopping model^[1, 19]:

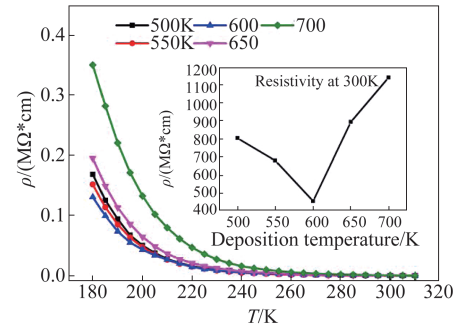


Fig. 3 Relations between electrical resistivity ρ and temperature T of MCNO films. The inset describes the electrical resistivity vs the deposition temperature, testing at 300 K.

图3 MCNO薄膜的电阻率与温度之间的关系,插图描述了在300 K下测试的电阻率和沉积温度的关系

$$\rho(T) = CT^\alpha \exp\left(\frac{T_0}{T}\right)^P, \quad (1)$$

where C is a temperature-independent constant, T_0 is the characteristic temperature in Kelvin, α and P are power-law exponents. To elucidate the character of hopping motion, the parameter P can be estimated from the negative slope of $\ln W$ vs $\ln T$. Where W is defined as^[23]:

$$W = \frac{1}{T} \frac{d(\ln \rho)}{d(T^{-1})} \approx -P \left(\frac{T_0}{T}\right)^P, \quad (2)$$

with ρ representing the resistivity of the MCNO films. Plots of $\ln W$ vs $\ln T$ for the films of different deposition temperatures are demonstrated in Fig. 4. For nearest neighbor hopping, $\alpha = P = 1$ ^[24]; while for variable-range hopping (VRH), $0.25 < P = \alpha/2 < 1$ ^[25]. As can be seen from the Fig. 4, in the range of 240 K to 310 K, the parameter P for the samples at different deposition temperatures are 0.40 ± 0.02 , 0.44 ± 0.03 , 0.47 ± 0.02 , 0.51 ± 0.02 and 0.41 ± 0.02 , respectively. The value of all the parameter P is around 0.5, which means that the small polaron hopping model can be elucidated to the VRH model^[18].

Figure 5(a) reveals the plots of $\ln(\rho/T)$ vs $1000/T^{0.5}$

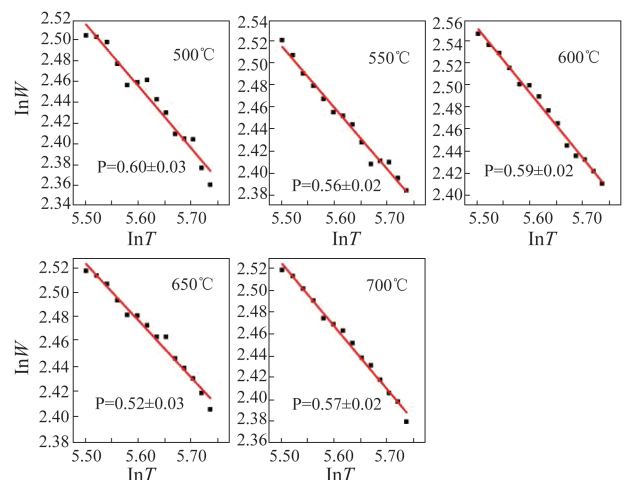


Fig. 4 Plots of $\ln W$ vs $\ln T$ for MCNO films of different deposition temperatures.

图4 不同沉积温度的MCNO薄膜 $\ln W$ 与 $\ln T$ 之间的关系

for MCNO films. The data of the samples have an ideal linear relation, which clearly ensures that the conductive type of MCNO films is standard VRH model.

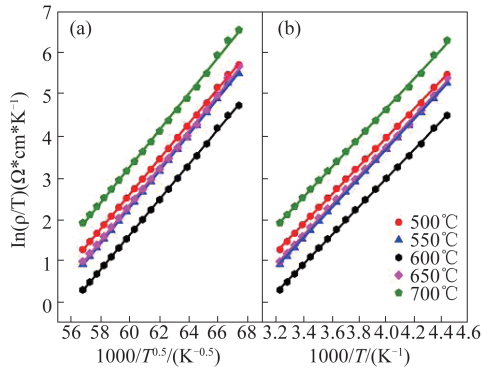


Fig. 5 Plots of $\ln(\rho/T)$ vs $1000/T^{0.5}$ (a), and $1000/T$ (b) for MCNO films of different deposition temperatures.

图 5 不同沉积温度 MCNO 薄膜的 $\ln(\rho/T)$ 与 $1000/T^{0.5}$ (a), $1000/T$ (b) 之间的关系

The relationship between temperature and resistivity can be demonstrated as [26]:

$$\ln(\rho/T) = \ln(k/[Nc(1-c)N_{\text{oct}}e^2d^2\nu_0]) + T_0/T = A + B/T \quad (3)$$

In this formula, $A = \ln(k/[Nc(1-c)N_{\text{oct}}e^2d^2\nu_0])$,

$B = T_0$, $E_A = kT_0$, $N = [\text{Mn}^{3+}] + [\text{Mn}^{4+}]$,

$Nc(1-c) = [\text{Mn}^{3+}] \times [\text{Mn}^{4+}] / ([\text{Mn}^{3+}] + [\text{Mn}^{4+}])$,

$c = [\text{Mn}^{4+}]_{\text{oct}} / ([\text{Mn}^{3+}]_{\text{oct}} + [\text{Mn}^{4+}]_{\text{oct}})$,

where e is the electronic charge, d is the hopping distance, ν_0 is the hopping frequency, T_0 is defined to be the system characteristic temperature and N_{oct} is the concentration per cm^3 of octahedral sites. The $Nc(1-c)$ factor denotes the probability that Mn^{3+} and Mn^{4+} occupy adjacent octahedral sites. From the formulas above, the characteristic temperature T_0 of the thin film materials can be obtained from the slopes of $\ln(\rho/T)$ vs $1000/T$ plots. The $\ln(\rho/T)$ vs $1000/T$ curves are plotted for the MCNO films at different deposition temperatures as exhibited in Fig. 5 (b). The characteristic temperature T_0 can be calculated from the slopes of $\ln(\rho/T)$ vs $1000/T$ plots. The energy required for small polarons to jump between Mn^{3+} and Mn^{4+} positions in the octahedral sites is reflected in the activation energy E_A . It can be computed through the formula: $E_A = kT_0$, where k is the Boltzmann's constant. Besides, for NTC material, temperature coefficient of resistance (TCR) is an undoubtedly important indicator for the performance of materials, and its value can be defined as:

$$\alpha = \frac{1}{R} \frac{dR}{dT} \quad (4)$$

The values of T_0 , E_A and α_{300} for MCNO films are listed in Table 1, where α_{300} is the TCR of the samples measured at 300 K.

Table 1 indicates that as the deposition temperature increases, both T_0 and E_A decrease first and then increase from 600 °C, which means that hopping of the small polarons between Mn^{3+} and Mn^{4+} is more active in the MCNO

Table 1 T_0 , E_A and α_{300} of MCNO films of different deposition temperatures

表 1 不同沉积温度 MCNO 薄膜的 T_0 , E_A 和 α_{300}

Deposition temperature/°C	T_0/K	E_A/eV	$\alpha_{300}/(\% \text{K}^{-1})$
500	3531	0.304	-3.727
550	3497	0.301	-3.774
600	3451	0.297	-3.829
650	3477	0.300	-3.780
700	3505	0.302	-3.732

films deposited at 600 °C. It is conspicuous to find that the values of T_0 , E_A and α_{300} are highly depended on the deposition temperature. In addition, the value of α_{300} at 600 °C is $-3.829 \% \text{K}^{-1}$, which means that the MCNO film has the best thermistor characteristics compared to other samples.

2.3 Magnetic properties

The temperature-dependent magnetization curves of MCNO films were measured during FC with an applied magnetic field of 10 000 Oe. As can be seen from Fig. 6, when the temperature increases, all the samples change from ferromagnetism to paramagnetism. The Curie temperatures T_c of the MCNO films deposited at 500 °C, 550 °C, 600 °C, 650 °C, 700 °C are 206 K, 209 K, 216 K, 211 K and 210 K, respectively. T_c has a maximum at 600 °C, which is suggestive of that the ferromagnetic coupling increases at first and then decreases as the deposition temperature increases [27]. The value of T_c is higher than the results (175~201 K) observed in MCNO films grown at different grown temperatures by CSD method [1, 6], but close to the T_c (210 K) of MCNO materials with high Co concentrations [28].

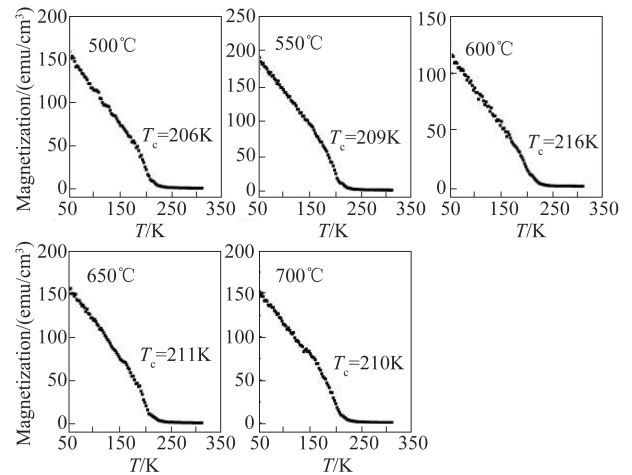


Fig. 6 Temperature dependence of magnetization ($M-T$) for MCNO films under 10 000 Oe recorded in FC mode

图 6 在 FC 模式 10 000 Oe 下 MCNO 薄膜磁化强度与温度的关系 ($M-T$)

Figure 7 exhibits the relations between $1/M$ and temperature T , in which the fitting curves are obtained by fitting the paramagnetic part of $1/M$ vs T curve with [6]:

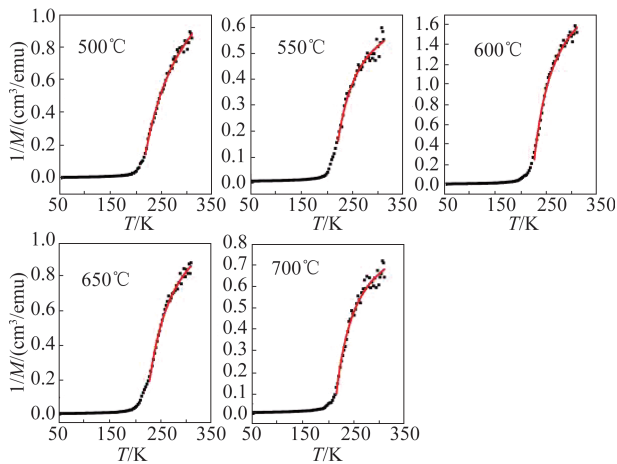


Fig. 7 Plots of the reciprocal magnetization vs temperature for MCNO films under 10 000 Oe recorded in FC mode
图7 在FC模式10 000 Oe下MCNO薄膜的磁化强度倒数与温度曲线

$$\chi = \chi_0 + \frac{C}{T + T_p} \quad (5)$$

where χ represents magnetic susceptibility, χ_0 represents non-paramagnetic contribution, T_p represents paramagnetic Curie temperature. Curie constant C lies in form of $C = N\mu^2/3k_B$, which can measure the paramagnetic ion concentration. N is the number of magnetic ions per gram, μ is the magnetic moment, and k_B is Boltzmann constant. The values of C , T_p and χ_0 are listed in Table 2. The magnetic susceptibility of the sample sharply grows after the ambient temperature increases to T_c . The decreasing value of C indicates a decrease in the number of paramagnetic ions. The T_p are negative values, which indicates that the coupling is ferromagnetic^[23]. As the deposition temperature increases, the absolute value of T_p increases at first and then decreases, which means the ferromagnetic coupling is enhanced at 600 °C. This phenomenon may be contributed by two reasons. First, the crystallization has a great dependence on deposition temperature, which can be proved by analyzing the AFM images. As the best crystallization appears at 600 °C, the grain growth leads to the enhancing of ferromagnetic coupling of the magnetic ions in the MCNO films, which can improve the ferromagnetic interaction^[6]. Second, the deposition temperature can affect the concentration of paramagnetic ions. The concentration of Mn^{2+} decreases at 600 °C, while the concentrations of Mn^{3+} and Mn^{4+} increases. Mn^{4+} can capture electrons from neighboring Mn^{3+} , and the hopping of the electrons is a double exchange process^[26, 29]. It leads to an increase in the conductivity of the MCNO films, which can be proved by the relations between electrical resistivity ρ and temperature T in Fig. 3. This can ensure a coupling that leads to ferromagnetism^[30].

3 Conclusions

In summary, a series of MCNO thin films with different deposition temperatures were successfully deposited on YSZ (100) substrates by PLD method. The crystalline quality of MCNO films is influenced by the deposi-

Table 2 C , χ_0 and T_p of MCNO films of different deposition temperatures

表2 不同沉积温度的MCNO薄膜的 C 、 χ_0 和 T_p

Deposition temperature/°C	$C/10^{-3} \text{ emu} \cdot \text{K} \cdot \text{cm}^{-3} \text{ Oe}$	$\chi_0/10^{-3} \text{ emu} \cdot \text{cm}^{-3} \text{ Oe}$	T_p/K
500	51.62±6.93	1.31±0.08	-190.36±2.33
550	39.04±3.53	1.07±0.05	-192.58±1.16
600	17.01±1.06	0.45±0.01	-201.71±0.79
650	31.09±2.52	0.77±0.03	-200.89±1.10
700	36.56±5.40	0.76±0.05	-198.62±3.22

tion temperature. From AFM images, the MCNO film deposited at 600 °C has the largest number of large-grains per unit area compared to other samples. By analyzing the electrical and magnetic data, the film with the deposition temperature of 600 °C has a large value of TCR (-3.829 %K⁻¹), low electrical resistivity (454.38 Ω·cm), and high Curie temperature (216 K). Accordingly, the investigations of the structural, electrical and magnetic properties illustrate that the deposition temperature of PLD system plays an important role in the performance of MCNO films.

Acknowledgment

This study was funded by the National Natural Science Foundation of China (61275111).

References

- [1] Hou Y, Huang Z M, Gao Y, *et al.* Characterization of $Mn_{1.56}Co_{0.96}Ni_{0.48}O_4$ films for infrared detection [J]. *Applied Physics Letters*, 2008, **92**(20): 202115.
- [2] Dannenberg R, Baliga S, *et al.* Resistivity, thermopower and the correlation to infrared active vibrations of $Mn_{1.56}Co_{0.96}Ni_{0.48}O_4$ spinel films sputtered in an oxygen partial pressure series [J]. *Journal of Applied Physic*.1999, **86**(1): 514–523.
- [3] Kong W W, Chen L, Gao B, *et al.* Fabrication and properties of $Mn_{1.56}Co_{0.96}Ni_{0.48}O_4$ free-standing ultrathin chips [J]. *Ceramics International*, 2014, **40**(6): 8405–8409.
- [4] Ma C, Ren W, Wang L, *et al.* Structural, optical, and electrical properties of $(Mn_{1.56}Co_{0.96}Ni_{0.48}O_4)_{1-x}(LaMnO_3)_x$ composite thin films [J]. *Journal of the European Ceramic Society*, 2016, **36**(16): 4059–4064.
- [5] Balakrishnan G, Tripura Sundari S, Ramaseshan R, *et al.* Effect of substrate temperature on microstructure and optical properties of nanocrystalline alumina thin films [J]. *Ceramics International*, 2013, **39**(8): 9017–9023.
- [6] Gao Y Q, Huang Z M, Hou Y, *et al.* Crystallization-dependent magnetic properties of $Mn_{1.56}Co_{0.96}Ni_{0.48}O_4$ thin films [J]. *Applied Surface Science*, 2010, **256**(8): 2552–2556.
- [7] Di W Q, Liu F, Lin T, *et al.* Influence of oxygen partial pressure on structural and electrical properties of $Mn_{1.56}Co_{0.96}Ni_{0.48}O_4$ thin films deposited by pulsed laser deposition [J]. *Applied Surface Science*, 2018, **447**: 287–291.
- [8] Zhou W, Zhang L, Ouyang C, *et al.* Micro structural, electrical and optical properties of highly (220) oriented spinel Mn–Co–Ni–O film grown by radio frequency magnetron sputtering [J]. *Applied Surface Science*, 2014, **311**(5): 443–447.
- [9] Xie Y, Ji G, Bu H, Kong W, *et al.* Effect of oxygen partial pressure and temperature on NTC characteristics of $Mn_{1.56}Co_{0.96}Ni_{0.48}O_4$ thin films grown on SrTiO₃ (100) by laser MBE [J]. *Journal of Alloys and Compounds*, 2014, **611**(2): 100–103.
- [10] Matsuyama T, Sakuda A, Hayashi A, *et al.* Preparation of amorphous TiS_x thin film electrodes by the PLD method and their application to all-solid-state lithium secondary batteries [J]. *Journal of Materials Science*, 2012, **47**(18): 6601–6606.

- [11] Yang P X, Meng X J, Huang Z M, *et al.* Ferroelectric polaron in layered perovskite ferroelectric thin films [J]. *Journal of Infrared and Millimeter Waves*, 2005, **24**(1): 1–6.
- [12] Pandis Ch, Brilis N, Tsamakos D, *et al.* Role of Low O_2 pressure and growth temperature on electrical transport of PLD grown ZnO thin films on Si substrates [J]. *Solid State Electronics*, 2005, **50**(6): 1119–1123.
- [13] Kong W W, Wei W, Gao B, *et al.* $\text{Mn}_{1.56}\text{Co}_{0.96}\text{Ni}_{0.48}\text{O}_{4\pm\delta}$ flexible thin films fabricated by pulsed laser deposition for NTC applications [J]. *Materials Science and Engineering B*, 2016, **206**: 39–44.
- [14] Ji G, Chang A, Xu J, *et al.* Low-temperature (<300 °C) growth and characterization of single-[100]-oriented Mn-Co-Ni-O thin films [J]. *Materials Letters*, 2013, **107**: 103–106.
- [15] Xie Y H, Kong W W, *et al.* Growth mode and properties of Mn-Co-Ni-O NTC thermistor thin films deposited on MgO (100) substrate by laser MBE [J]. *Modern Physics Letters, B*, 2014, **30**(28): 1450235.
- [16] He L, Ling Z Y, Huang Y T, *et al.* Effects of annealing temperature on microstructure and electrical properties of Mn-Co-Ni-O thin films [J]. *Materials Letters*, 2011, **65**(11): 1632–1635.
- [17] Wang J Y, Zhang J J. Structural and electrical properties of NiMg $_{1-x}$ Mn $_2$ O $_4$ NTC thermistors prepared by using sol-gel derived powders [J]. *Materials Science and Engineering B*, 2011, **176**(7): 616–619.
- [18] Zhou W, Wu J, Ouyang C, *et al.* Optical properties of Mn-Co-Ni-O thin films prepared by radio frequency sputtering deposition [J]. *Journal of Applied Physics*, 2014, **115**(9): 056601.
- [19] Kong W W, Bu H J, Gao B, *et al.* Effects of preferred orientation on electrical properties of $\text{Mn}_{1.56}\text{Co}_{0.96}\text{Ni}_{0.48}\text{O}_{4\pm\delta}$ spinel films [J]. *Materials Letters*, 2014, **137**: 36–40.
- [20] He L, Ling Z Y, Ling D X, *et al.* Role of film thickness on the microstructure and electrical properties of Mn-Co-Ni-O thin film thermistors [J]. *Materials Science and Engineering B*, 2015, **198**: 20–24.
- [21] Coey J M D, Viret M, Ranno L, *et al.* Electron localization in mixed-valence manganites [J]. *Physical Review Letters*, 1995, **75**(21): 3910–3913.
- [22] Park K, Bang D Y, *et al.* Electrical properties of Ni-Mn-Co-(Fe) oxide thick-film NTC thermistors prepared by screen printing [J]. *Journal of Materials Science: Materials in Electronics*, 2003, **14**: 81–87.
- [23] Ji G, Chang A M, Li H Y, *et al.* Epitaxial growth of Mn-Co-Ni-O thin films and thickness effects on the electrical properties [J]. *Materials Letters*, 2014, **130**: 127–130.
- [24] Efros A L, Shklovskii B I. Coulomb gap and low-temperature conductivity of disordered systems [J]. *Journal of Physics C: Solid State Physics*, 1975, **8**(11): L239–L240.
- [25] Schmidt R, Basu A, Brinkman A W, *et al.* Electron-hopping modes in NiMn $_2$ O $_{4\pm\delta}$ materials [J]. *Applied Physics Letters*, 2005, **86**(7): 325.
- [26] Wu J, Huang Z, Hou Y, *et al.* Structural, electrical, and magnetic properties of $\text{Mn}_{2.52-x}\text{Co}_x\text{Ni}_{0.48}\text{O}_4$ films [J]. *Journal of Applied Physics*, 2010, **107**(5): 256403.
- [27] Duan L B, Rao G H, Yu J, *et al.* Structural and magnetic properties of chemically synthesized $\text{Sn}_{1-x}\text{Mn}_x\text{O}_2$ nanocrystalline powders [J]. *Journal of Applied Physics*, 2007, **101**(6): 063917.
- [28] Peña O, Ma Y, Bahout M, *et al.* Structural and physical properties of spinel-type NiMn $_{2-x}$ Co $_x$ O $_4$ oxides [J]. *Physica Status Solidi (c)*, 2004, **1**(S1): S31–S34.
- [29] Punnoose A, Hays J, Gopal V, *et al.* Room-temperature ferromagnetism in chemically synthesized $\text{Sn}_{1-x}\text{Co}_x\text{O}_2$ powders [J]. *Applied Physics Letters*, 2004, **85**(9): 1559–1561.
- [30] Coey J M D, Viret M, von Molnár S. Mixed-valence manganites [J]. *Advances in Physics*, 2009, **58**(6): 571–697.